

Contents lists available at ScienceDirect

Catena

journal homepage: www.elsevier.com/locate/catena





Scenario analysis of high and steep cutting slopes protection in the loess hilly region: A case study of the Yangjuangou catchment in Yan'an, China

Zhi Cao ^{a,b}, Yurui Li ^{a,b,*}, Yansui Liu ^{a,b,*}, Yanxia Lu ^{c,d}

- ^a Institute of Geographic Sciences and Natural Resources Research, Chinese Academy of Sciences, Beijing 100101, China
- ^b Key Laboratory of Degraded and Unused Land Consolidation Engineering, Beijing 100101, China
- ^c China Land Surveying and Planning Institute, Beijing 100035, China
- ^d CAUPD Beijing Planning and Design Consultants Ltd., Beijing 100044, China

ARTICLE INFO

Keywords: Slope stability Soil erosion Land consolidation High and steep cutting slopes Scenario analysis The loess hilly region Loess plateau

ABSTRACT

Soil erosion and slope instability restrict the cutting slopes, especially the high and steep slopes of a construction site. It is difficult for present research of observation experiments and investigation to deal with these problems under climate change. Focusing on gully land consolidation in the loess plateau of China, this paper put forward a technical procedure to explore the optimal combination scheme of slope-cutting and vegetation-planting in future climate change. The technical procedure includes scenarios design, model calculation, and scheme optimization. This paper selected a back catchment in Yangjuangou catchment of Yan'an City as a case study and designed 54 combined scenarios consisting of 6 slopes, 3 types of vegetation (including bare land), and 3 climate scenarios. The soil erosion and slope stability under different scenarios were quantified using FLAC/Slope software and Water Erosion Prediction Project (WEPP) model. This paper innovatively designed elasticity inclores to trade off the increase of the flat land area formed by land consolidation and the resulting reduction in slope stability and increase in soil erosion. It is found that the slope of 53° with *Caragana microphylla* could be the optimal combination scheme considering flat land creating and the safety of slopes. The technical procedure and the resulting parameters could support gully land consolidation in related areas and be referenced by other construction projects.

1. Introduction

The ecological environment of a construction site (e.g., roads, railways, mining areas, and water conservancy engineering) is substantially disturbed, resulting in vegetation destruction, landscape degradation, soil loss, and landslide (Hancock et al., 2016; Wang et al., 2021). Specifically, the high and steep cutting slopes will cause serious soil erosion under rainfall conditions (Liu et al., 2019a; Ramos-Scharrón et al., 2022). A large number of high and steep cutting slopes were formed in large-scale land consolidation projects, such as the Gully Land Consolidation Project (GLCP) in Yan'an, China (Li et al., 2020b; Xu et al., 2021). The projects were to increase the available land area and balance economic development and eco-environmental protection by cutting off hilltops and filling gullies (Li et al., 2021; Liu et al., 2015). The GLCP

finished the construction of 2400 ha terraces and river-nearby farming lands, 658 silt dams, 2364 hydraulic structures, and 880 km of roads in 2014 (He, 2015). The safety of the high and steep cutting slopes formed following the project implementation has attracted wide attention (Li et al., 2014; Liu and Li, 2014).

Presently, researches on the safety and protection of high and steep cutting slopes include 5 aspects as followed: (1) Observation experiments on different excavation slopes with different vegetation types or ground covers to explore the optimal combination scheme. Lee et al. (2018) evaluated the effect of erosion control and vegetation establishment on steep slopes with seven mulch treatments (e.g., straw alone, straw with polyacrylamide, wood fiber, etc.). Feng et al. (2022) compared and analyzed the comprehensive effect of a combination of four vegetation styles and three levels of slope gradient. Liu et al.

Abbreviations: WEPP, Water Erosion Prediction Project; GGP, Grain for Green Project; GLCP, the Gully Land Consolidation Project; GPCC, Generator of Point Climate Change; CMIP6, Phase 6 of the Coupled Model Intercomparison Project; AR5, the IPCC's Fifth Assessment Report; RCPs, Representative Concentration Pathways; CMDC, China Meteorological Data Service Center; GCMs, Global Climate Models.

^{*} Corresponding authors at: Institute of Geographic Sciences and Natural Resources Research, Chinese Academy of Sciences, Beijing 100101, China. E-mail addresses: liyr@igsnrr.ac.cn (Y. Li), liuys@igsnrr.ac.cn (Y. Liu).

(2019a) investigated the efficiency of erosion control techniques on high stairstep cut-slopes, including vegetation coverage on platforms, counter-slope on platforms, upslope drainage, and comprehensive techniques. (2) Observation experiments on natural slopes with the combination of different land use or slope gradient to explore their role in soil and water conservation are carried out. Liu et al. (2019b) analyzed soil loss and runoff of different slope lengths in different land use. Jourgholami et al. (2021) examined the effect of slope gradient on runoff and sediment yield of ground-based skidding-operated land under natural rainfall conditions. (3) Investigation of properties of excavation slopes after gully land consolidation to explore factors of slope stability is another research area. Navarro-Hevia et al. (2016) studied soil erosion, sediment yield, and morphological evolution of railroad cut slopes. Jin et al (2019) investigated the water table and soil salinization in the region launching gully land consolidation. Shan et al. (2020) investigated soil moisture characteristics of the excavation slopes. (4) Research on characteristics of vegetation roots to select suitable vegetation draws great attention. Zhang et al. (2018) analyzed the effects of vegetation on soil erodibility on steep gully slopes. Liu et al. (2019c) studied the effects of root systems of planted and natural vegetation on rill detachment and erodibility of loess soil. (5) Examination of slope stability with modelling and stability analyses. Kaya et al. (2016) determined the effect on the stability of an existing landslide and planned slope excavations with limit equilibrium analyses. However, current studies focused more on slope degrees or vegetation types of excavation slopes with field experiments or surveys, suffering from comprehensive research on the optimal combination of slope degrees and vegetation of the cutting slopes in future climate change scenarios, which needed to be paid more attention to.

The goals of this paper were (i) to quantify soil erosion and slope stability of different slope-cutting and vegetation-planting schemes in future climate change scenarios and (ii) to explore the optimal combination scheme in the catchment of Yan'an, China. This study could provide technical parameters and processes for land consolidation in similar regions.

2. Methodology

2.1. Study area

The site of scenario analysis was conducted in Yangjuangou catchment (36°42́N, 109°31́E) located in northwestern Yan'an City, Shaanxi Province of China. The Yangjuangou catchment is a typical loess hilly and gully region of 3.11 km², running from north to south and dividing into two branches at the end (Cao et al., 2022). It has an elevation between 982 and 1250 m. The range of slope inclination is from 0° to 72°, and the average is 32°. The area is characterized by a semi-arid

continental monsoon climate, with annual precipitation of 550 mm. Rain and heat hit the area in the same seasons from July to September (Liu et al., 2017). In the struggle against soil erosion, the catchment has gone through the phases of afforestation, terraced fields construction, Grain for Green Project (GGP), and Gully Land Consolidation Project (GLCP). Since the late 1990s, the catchment has been an observation and research station for geographers and ecologists to research ecological restoration, water and soil conservation, land consolidation engineering technologies, optimization of land use patterns, sustainable land use mode, and regional transformation development (Feng et al., 2022; Fu et al., 1999; Liu and Li, 2017). The site was a small catchment in the back of the Yangjuangou catchment. It is bell-shaped with two slopes and one ditch. The slopes are about 120 m long and 12–15 m high with a gradient of 30°, and the ditch is about 20–100 m (Fig. 1).

2.2. Technical procedure

Slope degree, vegetation, and climate have important impacts on slope steady and gully safety. To explore the optimal combination scheme, this paper sets slope, vegetation, and climate scenarios, and comprehensively considers the area of the flat land area formed by land consolidation, and the resulting reduction in slope stability and increase in soil erosion. The three aspects and their relationship were quantitatively analyzed with safety factor, erosion modulus, and the flat land area elasticity of safety factor and that of erosion modulus. The safety factor is the ratio of available shear strength to the strength required to maintain stability (Murthy, 2003; Samtani and Nowatzki, 2006), which was used to reflect slope stability. The erosion modulus is the amount of soil erosion per unit area per unit time (Ma et al., 2019), which was used to reflect the soil erosion intensity. The flat land area elasticity of safety factor is the ratio of the increase in the flat land area to the increase in the safety factor, and similarly, the flat land area elasticity of erosion modulus is the ratio of the increase in the flat land area to the increase in the erosion modulus. The two elasticity indicators are designed to reflect the relationship between the flat land area and the ecological effects (i. e., slope stability, and soil erosion). The two elasticity indicators were designed to measure how sensitive the soil erosion or slope instability is to the excavated flat land area as the slope inclination increases.

In the analysis, the FLAC/Slope software, GPCC (Generator of Point Climate Change) program, and WEPP model were used (Fig. 2). The FLAC/Slope software is a special, streamlined version of FLAC for evaluating the factor of safety of soil and rock slopes, widely used in international geotechnical communities to reflect slope stability (Chugh et al., 2007). Many research directly used the FLAC/Slope software in calculating the safety factor of high and steep slopes (Satyanarayana et al., 2021; Singh et al., 2013). The calculation of the safety factor of slopes needed geometry and parameters of slopes, including slope

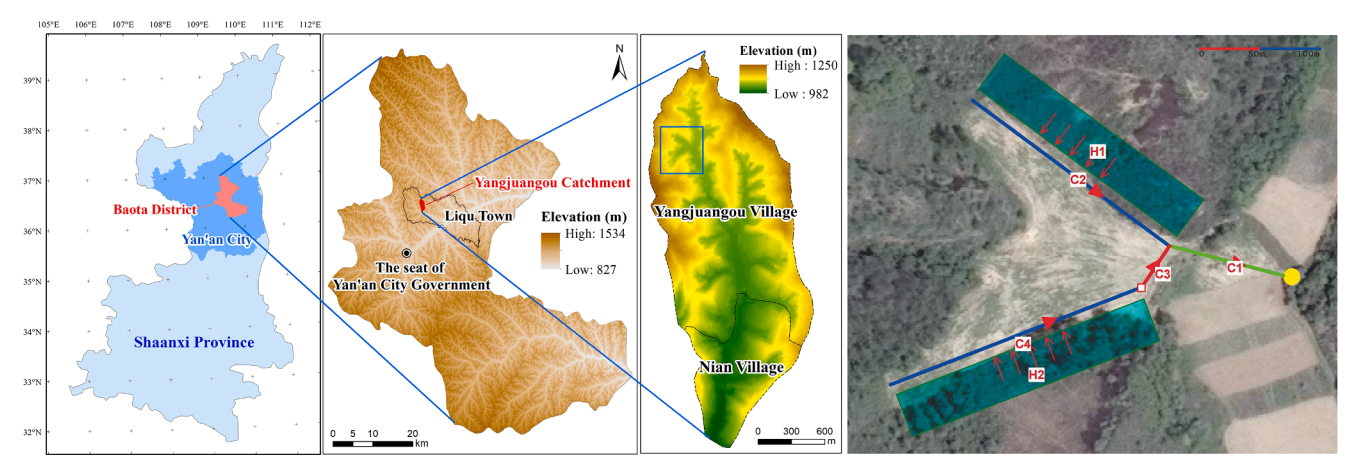


Fig. 1. Location of the study catchment and its layout of slopes and ditch.

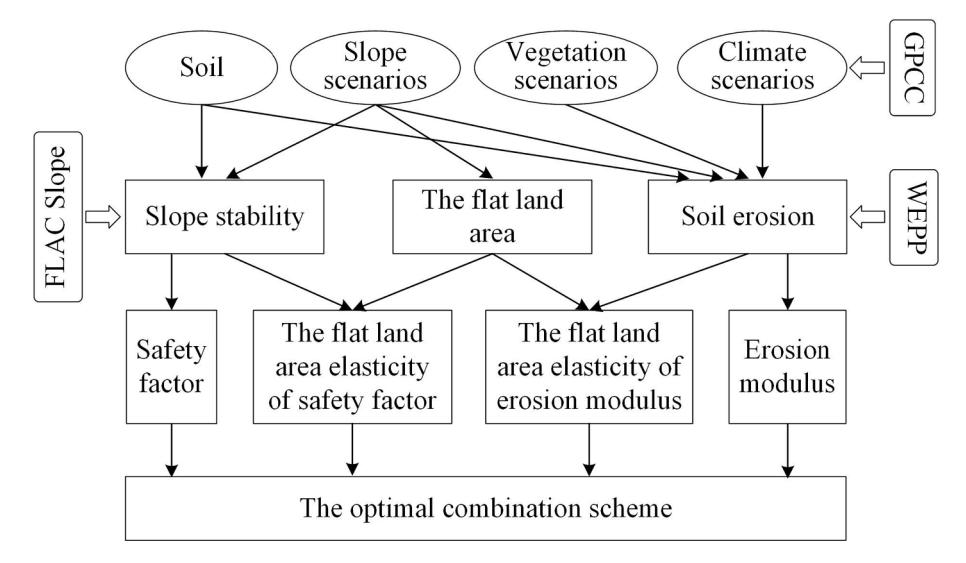


Fig. 2. The technical procedure to explore the optimal combination scheme.

profile, soil layers, and their soil properties (like unit weight, cohesion, and internal friction angle). The WEPP model is a process-based and continuous simulation model including climate, surface and subsurface hydrology, winter processes, irrigation, plant growth, and residue decomposition, developed for application to estimate soil erosion from hillslope profiles and small watersheds (Nearing et al., 1989). The WEPP model performed very well on small watershed sites (Laflen et al., 1997; Flanagan et al., 2012; Douglas-Mankin et al., 2020). The GPCC program (https://github.com/Jiechenwhu/GPCC/) is a downscaling software program that could effectively downscale climate model-simulated monthly precipitation and temperature at grid box scales to daily time series at a station scale around the world (Chen et al., 2018).

2.3. Scenarios for climate, slope, and vegetation

This paper set scenarios from climate change, slope gradient, and vegetation protection to find the prioritization combination scheme (Fig. 3).

Due to the instability of the data from Phase 6 of the Coupled Model Intercomparison Project (CMIP6), the climate change scenarios adopted the set of scenarios in the IPCC's Fifth Assessment Report (AR5). The scientific community of the report has defined a set of four scenarios, denoted Representative Concentration Pathways (RCPs) which refers to approximate total radiative forcing in the year 2100 relative to 1750. The RCPs include one low scenario (RCP2.6), two intermediate

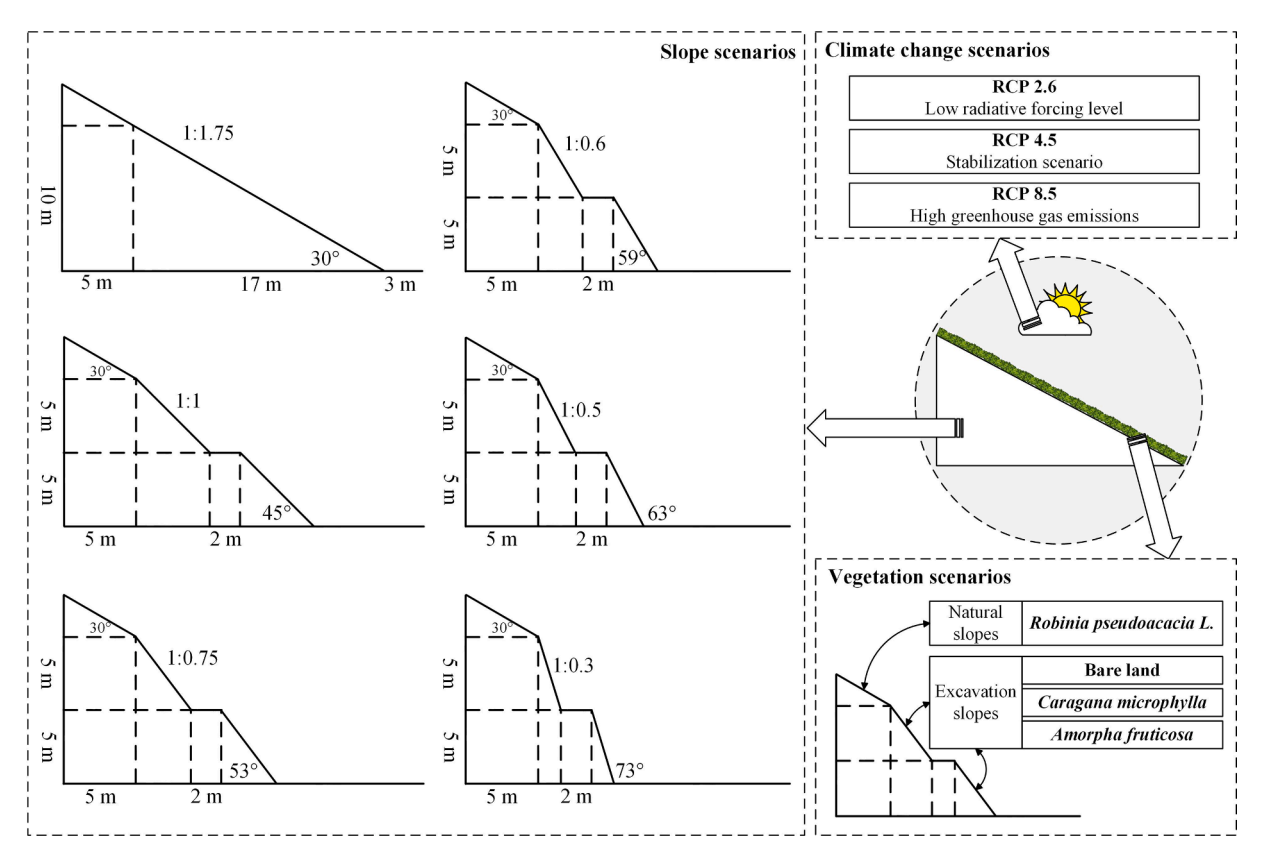


Fig. 3. Scenarios of climate change, slope and vegetation for soil erosion.

stabilization scenarios (RCP4.5 and RCP6), and one high scenario (RCP8.5) (IPCC, 2013). Due to part of the climate models didn't simulate the scenario of RCP6 which belonged to the same stabilization scenarios as that of RCP4.5, this paper used the scenarios of RCP2.6, RCP4.5, and RCP8.5 to indicate the climate characteristics during 2020–2050.

Six levels of slope gradient were chosen, including $30^\circ, 45^\circ, 53^\circ, 59^\circ, 63^\circ, 73^\circ, or 1:1.75, 1:1, 1:0.75, 1:0.6, 1:0.5, 1:0.3 in slope ratio form. The slope with <math display="inline">45^\circ, 53^\circ, 59^\circ, 63^\circ,$ and 73° added platform design between slopes which was consistent with gully land consolidation practices. The platform was 2 m wide, and the two slopes above and below the platform were 5 m high. A natural slope of 30° was retained above the second slope with a bottom width of 5 m.

Vegetation types for excavation slope protection were set to *Caragana microphylla* and *Amorpha fruticosa*, which are commonly planted for slope protection (Xue et al., 2009; Song et al., 2014). Bare land was also included in the excavation slope protection type for comparison purposes. The vegetation of the natural slope was retained *Robinia pseudoacacia L*.

2.4. Data source and processing

2.4.1. Climate data

The climate data during 2020–2050 needed by the WEPP model was simulated by the CLIGEN model considering the availability of climate data. The CLIGEN model is a stochastic weather generator. It could estimate daily time series precipitation, temperature, dewpoint, wind, and solar radiation for a single geographic point with monthly climate parameters (means, standard deviation, skewness, etc.). The dataset of the model included monthly climate parameters data of more than 2600 US stations as .par files. Finding a matching station with similar climate features to the study area and replacing corresponding climate parameters was proved to be an effective way to use the CLIGEN model outside the USA (Zhang, 2004; Miao et al., 2004; Liu et al., 2013). And the realization of this method requires the matching station and estimated daily precipitation, maximum and minimum temperature data during 2020–2050 in the new version of the WEPP model.

Matching station determination is conducted in three steps. Firstly, it is to select US stations whose annual precipitation was within the mean \pm standard deviation of annual precipitation in the Yangjuangou catchment during 1971–2005. The mean and standard deviation of annual precipitation was 513.54 mm and 111.89 mm, and 353 US stations met precipitation requirements. In particular, the time range of the annual precipitation was determined by the time range of the historical data of CMIP5 and that of the daily meteorological observation data of Yan'an station. Then, the correlations between the monthly precipitation of the Yangjuangou catchment and 353 US stations are analyzed. Finally, the matching station is determined based on the maximum coefficient of determination (R²). The BAUDETTE 21SSE station in Minnesota was the selected matching station with the largest $R^2=0.94$.

The estimated daily precipitation, maximum and minimum temperature data during 2020–2050 was produced by the GPCC, by inputting data including the observed daily precipitation, maximum temperature, and minimum temperature in Yangjuangou catchment during 1971–2005, and Global Climate Model-simulated monthly precipitation, maximum temperature, and minimum temperature during 1971–2005 and that of three climate scenarios (RCP2.6, RCP4.5, and RCP8.5) during 2020–2050.

The daily climate parameters (precipitation, maximum temperature, and minimum temperature) during 1971–2005 were the daily meteorological observation data of Yan'an station (one of the national primary standard weather stations) from the dataset of daily climate data from Chinese surface stations for global exchange (V3.0) obtained from China Meteorological Data Service Center (CMDC) (https://data.cma.cn/). The monthly precipitation and temperature parameters of three climate scenarios (RCP2.6, RCP4.5, and RCP8.5) during 1971–2005 and 2020–2050 were the monthly climate simulation data of the Global

Climate Models (GCMs) extracted with the latitude and longitude of the Yangjuangou catchment. This paper used the average of the simulation results of 8 commonly Global Climate Models (Table 1) to ensure the data credibility. The climate simulation data was obtained from the IPCC Data Distribution Centre (https://www.ipcc-data.org/).

2.4.2. Soil properties

The soil type of the slopes is loess of Malan, and its major chemical and physical properties are shown in Table 2. The soil parameters of particle size, soil texture, organic matter, CEC, and critical shear were measured with soil samples and updated in the soil component of the WEPP model (Feng et al., 2022). The soil parameters of interrill erodibility, rill erodibility, and effective hydraulic conductivity were calculated based on the soil parameters of particle size and CEC with the WEPP model. Other soil parameters kept that of the WEPP.

The unit weight was measured with the cutting ring method, and the cohesion and internal friction angle of the slopes were measured with the triaxial compression test (Shinohara et al., 2000; Zhang et al., 2010). These properties were used to calculate the slope stability safety factor using FLAC/Slope software. When the factor of safety is 1.0, the slope is said to reach limit equilibrium. If it is less than 1.0, a landslide occurs since the available shear strength exceeds the strength required to maintain stability. When it is slightly higher than 1.0, the slope is stable but a small disturbance (e.g., an earthquake) may lead to a landslide (Murthy, 2003; Samtani and Nowatzki, 2006). The larger the factor of safety, the more stable the slope.

2.4.3. Plant parameters

The 10 plant parameters of *Caragana microphylla*, *Amorpha fruticosa*, and *Robinia pseudoacacia L* in Fig. 3 were referred to relative research (Du, 2013; Huang, 1986; Liang and Long, 2010; Niu, 2003; Yin et al., 2008). And the 8 initial condition parameters of those three vegetations were set according to the practical situation and updated in the plant growth component of the WEPP model. The other plant parameters and initial parameters needed were default values in the WEPP model plant database (Table 3). Specifically, all the other plant parameters of *Caragana microphylla* and *Amorpha fruticosa* were based on the Shrub-Perennial, and those of *Robinia pseudoacacia L* were based on the Forest-Perennial in the WEPP model plant database. Besides, all the parameters of bare land were based on the Cut Slope in the WEPP model plant database.

The data of three climate scenarios, soil properties, and the attributes of four plants were inputted into the WEPP model to simulate soil erosion under combined scenarios with different climate scenarios, gradients of slopes, and vegetation types in the next 30 years (during 2020–2050).

Table 1Feature information of 8 Global Climate Models.

No.	Model	Country	Resolution (Lat/ lon)	Time
1	BCC-	China	2.8°×2.8°	1971–2005,
	CSM1.1			2020-2050
2	BNU-ESM	China	$2.8^{\circ} \times 2.8^{\circ}$	1971–2005,
				2020-2050
3	CCSM4	USA	$0.9^{\circ} \times 1.3^{\circ}$	1971–2005,
				2020-2050
4	CNRM-CM5	France	$1.4^{\circ} \times 1.4^{\circ}$	1971–2005,
				2020-2050
5	GFDL-CM3	USA	$2.0^{\circ} \times 2.5^{\circ}$	1971–2005,
				2020-2050
6	MIROC5	Japan	$1.4^{\circ} \times 1.4^{\circ}$	1971–2005,
				2020-2050
7	MPI-ESM-	Germany	$1.9^{\circ} \times 1.9^{\circ}$	1971–2005,
	LR			2020-2050
8	NorESM1-M	Norway	$1.9^{\circ} \times 2.5^{\circ}$	1971–2005,
				2020–2050

 Table 2

 Soil properties of the slopes in Yangjuangou catchment.

Particle S Sand	Size (%) Silt	Clay	Soil Texture	Organic Matter (%)	CEC (Cmol kg ⁻¹)	Rill Erodibility (s m ⁻¹)	Critical Shear (Pa)	Unit Weight (kN m ⁻³)	Cohesion (kPa)	Internal Friction Angle (°)
24.1	69.7	6.2	Silty loam	1.34	10.73	0.0235	3.84	18.32	12.55	23.5

Table 3The parameters of vegetation.

Parameter	Units	Value			
		Bare land	Caragana microphylla	Amorpha fruticosa	Robinia pseudoacacia L
Plant parameter					
In-row plant spacing	cm	(499.9)	100	100	200
Plant stem diameter at maturity	cm	(0.1)	1.3	10	60
Base daily air temperature	Degrees C	(2)	5	5	7.1
Maximum temperature that stops the growth of a perennial crop	Degrees C	(32)	45	41.3	(40)
Critical freezing temperature for a perennial crop	Degrees C	(-40)	(-40)	-38.89	-26
Maximum canopy height	cm	(15)	100	150	2000
Maximum leaf areas index		(1)	1.195	1.882	10.5
Maximum root depth	cm	(10)	400	150	300
Root to shoot ratio	%	(33)	600	184	58.33
Maximum root mass for a perennial crop	Kg m ⁻²	(0.001)	1.61	1.61	1.59
Initial condition parameter					
Initial canopy cover	%	(0)	0	0	90
Days since last tillage	days	(0)	1000	1000	0
Days since last harvest	days	(0)	1000	1000	0
Cumulative rainfall since last tillage	mm	(0)	1000	1000	0
Initial interrill cover	%	(0)	0	0	100
Initial rill cover	%	(0)	0	0	100
Initial total dead root mass	kg m ⁻²	(0)	0	0	1.59
Initial total submerged residue mass	kg m ⁻²	(0)	0	0	1.59

Note: the data within the parentheses was default values in the WEPP model plant database.

2.5. The elasticity indicators

2.5.1. The flat land area elasticity of safety factor

Measuring the relationship between slope stability and the flat land area as the slope of the excavation slope increases is pivotal to getting the prioritization combination scheme. The elasticity indicator quantifies the relative change relationship between two variables (Browning and Zupan, 2020). This paper set the flat land area elasticity of safety factor, which is the percentage change in the safety factor to that in the flat land area. The flat land area elasticity of safety factor could indicate how sensitive the safety factor of the excavation slope is to the increase in the flat land area. The smaller the value of the indicator when it is less than 1.0, the slower the decrease in the safety factor is than the increase in the flat land area. The larger the value of the indicator when it is greater than 1.0, the faster the decrease in the safety factor is than the increase in the flat land area. If the value of the indicator suddenly increases as the slope inclination increases, it means the increase in slope inclination brings about a larger change in slope stability.

2.5.2. The flat land area elasticity of erosion modulus

Similarly, to measure the relationship between soil erosion and the flat land area as the slope of the excavation slope increases is also important to explore the optimal combination scheme. This paper also designed the flat land area elasticity of erosion modulus, which is the ratio of the percentage change in erosion modulus to that in the flat land area. The flat land area elasticity of erosion modulus could evaluate how sensitive the erosion modulus of the excavation slope is to the increase in the flat land area. The smaller the absolute value of the indicator when it is less than 1.0, the slower the increase/decrease in the erosion modulus is than the increase in the flat land area. The larger the absolute value of the indicator when it is greater than 1.0, the faster the increase/decrease in the erosion modulus is than the increase in the flat land area. If the value of the indicator suddenly increases as the slope inclination increases, it means the increase in slope inclination brings about a larger

change in soil erosion.

3. Results

3.1. Precipitation and temperature

The predicted annual precipitation under three climate change scenarios (i.e., RCP 2.6, RCP 4.5, and RCP 8.5) during 2020–2050 are 555.02 mm, 550.89 mm, and 550.75 mm, respectively. Those are 41.48 mm, 37.35 mm, and 37.21 mm higher than the historical measured data (513.54 mm during 1971–2005). Under the three scenarios, the precipitation in most months increases variously compared to historical periods, and the decrease in precipitation is mainly in August. The months with increasing precipitation are June and July under the climate change scenario of RCP 2.6, May and July under the climate change scenario of RCP 4.5, and September under the climate change scenario of RCP 8.5 (Fig. 4).

Each month average of the predicted daily maximum and minimum temperature under the three scenarios during 2020–2050 is higher than that during 1971–2005. The predicted daily maximum temperature under the scenarios of RCP 2.6, RCP4.5, and RCP 8.5 meanly increase by $1.47^{\circ}\text{C}, 1.54^{\circ}\text{C},$ and $1.78^{\circ}\text{C},$ respectively. Those are $1.50^{\circ}\text{C}, 1.61^{\circ}\text{C},$ and 1.93°C in terms of the predicted daily minimum temperature. The months with faster temperature increase are August, September, and December, while the slower increase was found in March, April, and May (Fig. 5).

3.2. Soil erosion

The erosion modulus of the bare slopes decreases with the increase of slope inclination under the 3 climate change scenarios, but that of the vegetated slopes showed an inverse trend. The predicted erosion modulus presents RCP 2.6 > RCP 4.5 > RCP 8.5 regardless of vegetation coverage on the slope. Amorpha fruticosa and Caragana microphylla

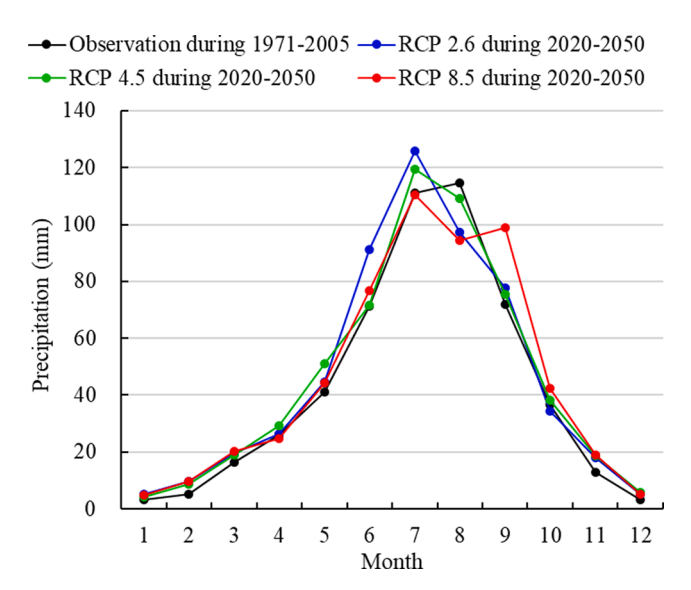


Fig. 4. The predicted precipitation of the study catchment.

can reduce most soil erosion according to the ratio of the runoff modulus of the vegetated slopes to that of the bare slopes in the corresponding degree. *Caragana microphylla* demonstrated a stronger ability of soil

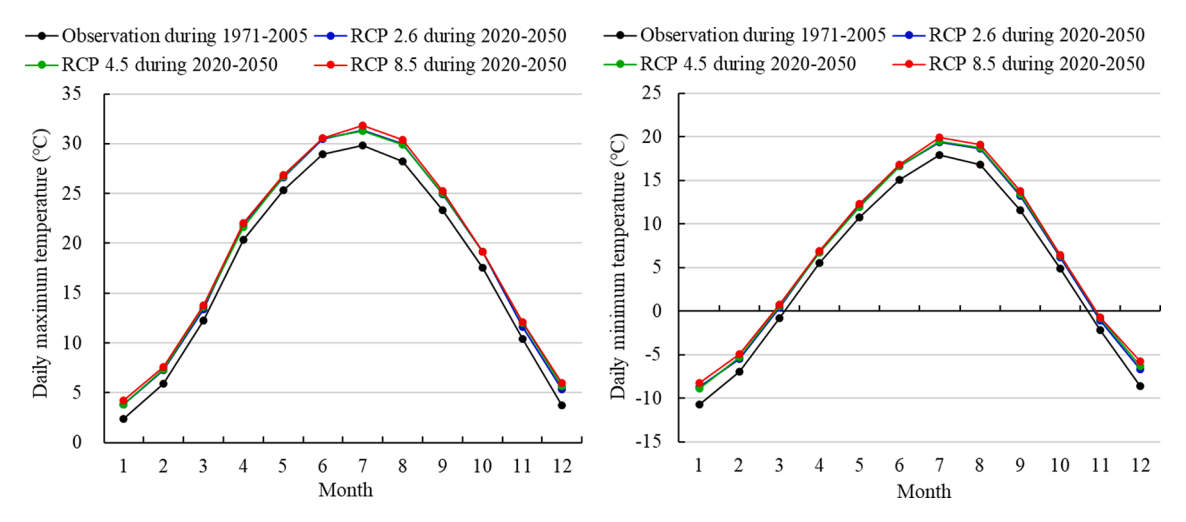
conservation than *Amorpha fruticosa*. Furthermore, the total soil erosion of slopes with vegetation protection increased with the increase in slope inclination, but the net soil erosion was just the opposite (Fig. 6 and Table 4).

The value of the flat land area elasticity of erosion modulus increases continuously as the slope with vegetation increases. Most of the values of the elasticity are less than 1. When the slope is less than 53° , the value of the elasticity changes slightly. When the slope is larger than 53° , that changes significantly under the climate scenarios of RCP 2.6 and RCP 8.5. It indicates that the soil erosion caused by the increases in the excavation slope increases significantly when the slope is greater than 53° (Table 5).

3.3. Slope stability

Table 6 shows the value of the safety factor of the 6 slopes. The value of the safety factor decreases with the increase of slope inclination. The safety factors of the slopes with inclinations below 73° are higher than 1.0. Only the safety factors of the slopes with 73° inclination are lower than 1.0, indicating those are unstable.

Table 7 shows the value of the flat land area elasticity of safety factor. The absolute value of the elasticity continues to increase with the increase of slope inclination. All the absolute values of the elasticity are less than 1. The absolute values of the elasticity with slope inclination above 53° are higher than those values with slope inclination below 53° .



 $\textbf{Fig. 5.} \ \ \textbf{The predicted temperature of the study catchment.}$

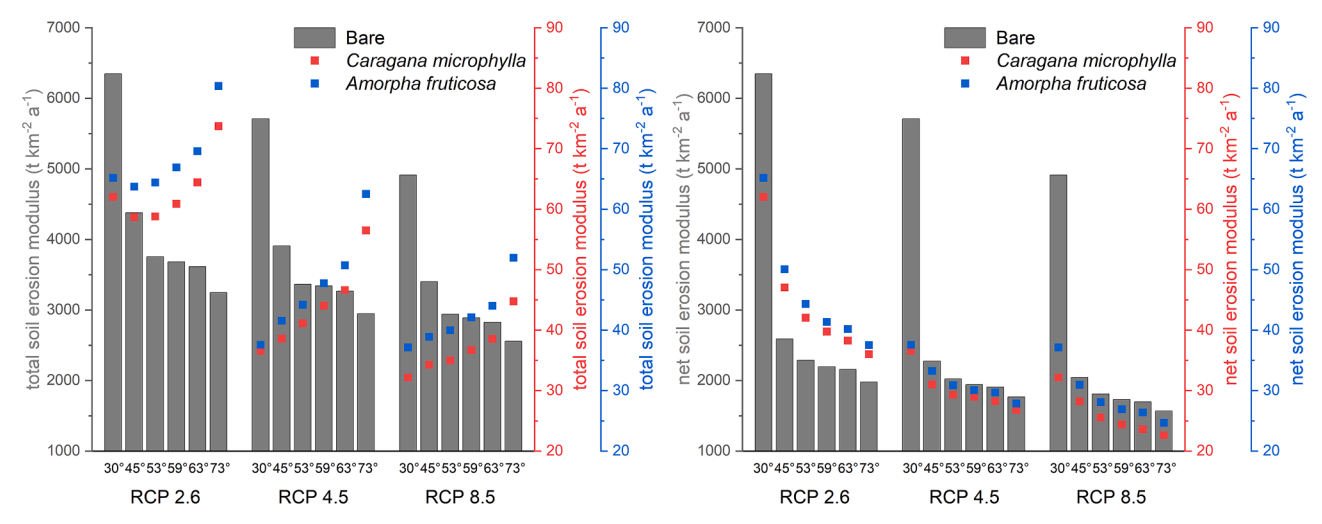


Fig. 6. The total and net soil erosion modulus of different climate, vegetation and slope inclination scenarios.

Table 4The total erosion modulus of different climate, vegetation and slope inclination scenarios.

Slope	Slope RCP 2.6 (t km ⁻² a ⁻¹)			RCP 4.	5 (t km ⁻² a ⁻¹)		RCP 8.	RCP 8.5 (t km ⁻² a ⁻¹)		
inclination	Bare	Caragana microphylla	Amorpha fruticosa	Bare	Caragana microphylla	Amorpha fruticosa	Bare	Caragana microphylla	Amorpha fruticosa	
30°	6346	62.03	65.17	5708	36.56	37.56	4913	32.17	37.14	
45°	4379	58.68	63.71	3908	38.60	41.56	3402	34.28	38.87	
53°	3754	58.79	64.42	3365	41.11	44.19	2940	35.00	39.98	
59°	3681	60.89	66.90	3341	44.06	47.76	2886	36.71	42.12	
63°	3615	64.43	69.59	3267	46.63	50.72	2827	38.56	44.03	
73°	3247	73.73	80.37	2948	56.50	62.53	2557	44.76	51.94	

Table 5The flat land area elasticity of total soil erosion modulus of different climate and vegetation scenarios under the increase of slope inclination.

increase of slope	RCP 2.	6		RCP 4.	5		RCP 8.	RCP 8.5		
inclination	Bare	Caragana microphylla	Amorpha fruticosa	Bare	Caragana microphylla	Amorpha fruticosa	Bare	Caragana microphylla	Amorpha fruticosa	
30°→45°	-0.19	-0.03	-0.01	-0.19	0.03	0.06	-0.18	0.04	0.03	
45°→53°	-0.46	0.01	0.04	-0.44	0.21	0.20	-0.43	0.07	0.09	
53°→59°	-0.14	0.25	0.27	-0.05	0.50	0.57	-0.13	0.34	0.38	
59°→63°	-0.22	0.70	0.48	-0.27	0.70	0.75	-0.25	0.60	0.54	
63°→73°	-0.66	0.94	1.01	-0.63	1.38	1.51	-0.62	1.05	1.17	

It indicates that the slope stability caused by the increases in the excavation slope decreases obviously when the slope is greater than 53° , especially when the slope increase from 53° to 59° .

4. Discussions and implications

4.1. The optimal combination scheme

From the perspective of slope stability, the slopes with inclination below 63° are safe for their safety factors higher than 1.0. If both slope stability and the flat land area are considered (i.e., from the value of the flat land area elasticity of safety factor), the slopes with 53° inclination are better than those with 63° with less safety factor reduction and increasing more flat land area. From the perspective of soil erosion, the soil erosion of slopes with vegetation protection is reduced significantly. Under the three climate scenarios, the erosion modulus of all the vegetation-protected slopes with different inclinations are lower than the allowable erosion modulus. In terms of coupling analysis of soil erosion and the flat land area (i.e., from the value of the flat land area elasticity of total soil erosion modulus), the slopes with 53° inclination achieve more flat land area but a slight soil erosion increase. The soil erosion of slopes with Caragana microphylla is also slightly less than that of slopes with Amorpha fruticosa with the same slope inclinations in the three climate scenarios. Therefore, the slope of 53° with Caragana microphylla could be the optimal combination scheme. That may be related to the precipitation of different climate change scenarios. In fact, this paper focuses more on exploring the set of technical procedures for the optimization of slope protection and ditch-slope utilization. In the planning and design for land consolidation projects in similar regions, optimizing the scheme requires consideration of more detailed observed data of soil properties, soil layers, and precipitation according to the

Table 6The safety factor of slope stability of different slope inclination.

Slope	30°	45°	53°	59°	63°	73°
Safety Factor	1.787	1.471	1.322	1.193	1.127	0.979

Table 7The flat land area elasticity of safety factor of different slope inclination.

Slope	$30^{\circ}{ o}45^{\circ}$	45°→53°	53° →59°	59°→63°	63°→73°
Safety Factor	-0.11	-0.32	-0.68	-0.66	-0.85

technical procedures.

4.2. Model validation and comparative analysis

It is verified that the WEPP model could be used to calculate the soil loss of steep slopes. This paper used stairstep cut-slope experimental data in Liu et al. (2019a) research to validate the WEPP model. The experimental plots, 16.6 km far from the Yangjuangou catchment, were a total height of 55 m with two sections. The upper 30 m section was a 45° slope left undisturbed with natural vegetation, and the lower 25 m section was cut at a 60° slope with a stairstep cut-slope. The research designed five plots including treatments of vegetation coverage, counter-slope, upslope drainage, bare land, and comprehensive techniques. The observed data used to validate the WEPP model was sediment loss with storms in the bare land plot. Simulated data with the WEPP model was similar but had a slightly higher rate of trends than observed data (Fig. 7).

Simulated results (e.g. climate change trends, erosion modulus of different slope inclination and vegetation planting, the optimal slope inclination) were consistent with the field experiments and relative research of the same catchment or nearby catchment (Feng et al., 2022; Liu et al., 2019b,a, 2022; Shi et al., 2018; Zhang et al., 2021; Hou and

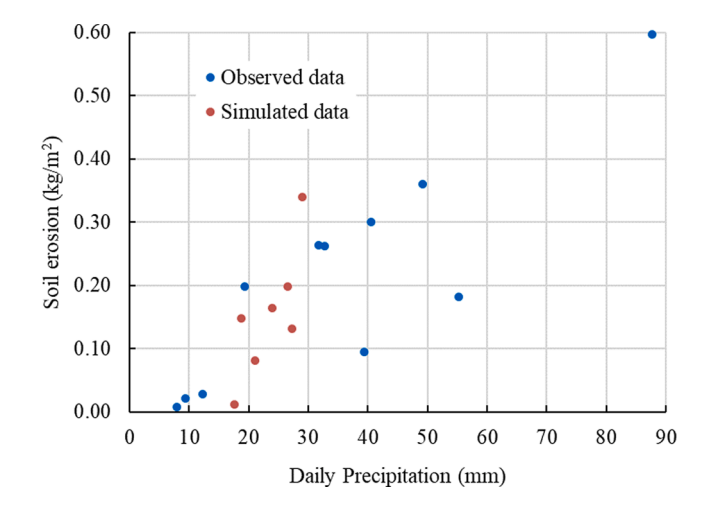


Fig. 7. The observed and the simulated data of a stairstep cut-slope experimental plot.

Cao, 1990).

Firstly, the paper found the future climate showed a trend of "warm and humid", consistent with other studies (Gao et al., 2017; Hu et al., 2020; Wang et al., 2020). Normally, the simulation and prediction of future climates are highly complex uncertainty (Taylor et al., 2012). The way to reduce uncertainty generally includes calculating the average of prediction data of many GCMs and adopting temporal or spatial downscaling methods (Gao et al., 2017; Zhang and Liu, 2005). We selected 8 GCMs and a GPCC downscaling program and found the study area would be "warm and humid" in the future, in line with current studies (Gao et al., 2017; Hu et al., 2020; Wang et al., 2020).

Secondly, the erosion modulus in this paper was the same order of magnitude as the findings of field experiments (Liu et al., 2019b, 2022; Shi et al., 2018; Zhang et al., 2021; Hou and Cao, 1990). Liu et al. (2019b) observed that the net soil erosion modulus of bared cutting-slope with 60° inclination was about 2300 t km 2 a 1 . Liu et al. (2022) mentioned the Yangjuangou catchment the erosion was 3270 t km 2 a 1 . Shi et al. (2018) found that the two runoff plots with grassland were 170 \pm 42 t km 2 a 1 and 327 \pm 42 t km 2 a 1 respectively. Furthermore, this paper found the soil loss of slopes with *Caragana microphylla* is less than those with *Amorpha fruticosa*. This result is consistent with the finds that *Caragana microphylla* has better anti-erodibility and soil preserving capability than *Amorpha fruticosa* in related studies (Xue et al., 2009; Wei et al., 2004).

Thirdly, this paper found that the soil erosion of the slopes with *Amorpha fruticosa* was higher than that of the slopes with *Caragana microphylla*, which was consistent with the findings of the field experiment 24.0 km far from the Yangjuangou catchment (Xue et al., 2009). Xue et al. (2009) tested the anti-erodibility of five vegetation restoration models and found that the anti-erodibility with *Caragana microphylla* was better than that with *Amorpha fruticose*. The soil anti-erodibility indices of *Caragana microphylla* was 0.7804, and that of *Amorpha fruticose* was 0.7516 or 0.6383. Wei et al. (2004) also found the soil and water conservation of *Caragana microphylla* was better than that of *Amorpha fruticose*. The ecological efficiencies of water-retaining and soil-retaining of *Caragana microphylla* were 10650–21300 and 439.5 RMB hm⁻² respectively, and those of *Amorpha fruticose* were 2291.7–4583.4 and 54.9 RMB hm⁻² respectively.

Fourthly, the optimal slope inclination (i.e. 53°) found with the elasticity indicators was consistent with the findings of the field experiment in the same catchment (Feng et al., 2022). Feng et al. (2022) designed experimental plots of single slopes with three inclinations (45°, 53°, 63°) and four vegetation styles (bare land, *Caragana microphylla*, *Amorpha fruticosa*, and mixed *C. microphylla* and *A. fruticosa*) and analyzed the comprehensive benefit of the experimental plots with vegetation growth index, soil erosion index, and engineering benefit index. They found the comprehensive benefit index of the slope with 53° was 5.8, greater than that of slopes with 45° and 63°, which were 3.9 and 4.0 respectively. The elasticity indicators mainly used to be applied in economics (Browning and Zupan, 2020), not in the field of water and soil conservation. This paper introduced the elasticity indicators to tradeoff the acquired flat land and the ecological effects of slope, getting expected results.

4.3. The changes in the soil erosion

The bare or vegetation-protected slopes have similar changing characteristics of soil erosion with increasing slope inclination under different climate change scenarios. The soil erosion of the bare land decreased with the increase of slope inclination but that of the vegetation-protected slope increased. That may be related to the critical slope gradient for erosion, varying from $10^{\circ}-30^{\circ}$ with different slope properties (Jiang et al., 2014; Jourgholami et al., 2021; Qian et al., 2016; Li et al., 2020a). It could be seen that the slope inclination of this research reaches the critical slope gradient, and the soil erosion of the bare slopes no longer increases as the increase in slope gradient but

shows a decreasing trend. For example, the total erosion modulus of the bare slopes decreased from 6346 t km $^{-2}$ a $^{-1}$ to 3247 t km $^{-2}$ a $^{-1}$ under the climate change scenario of RCP 2.6. The erosion resistance of vegetation decreases with the increase in slope inclination, resulting in an increase in soil erosion (Mohammad and Adam, 2010; Wang et al., 2017). For example, the total erosion modulus of the vegetation-protected slopes with Caragana microphylla increased from 36.56 t km $^{-2}$ a $^{-1}$ to 56.50 t km $^{-2}$ a $^{-1}$ under the climate change scenario of RCP 4.5.

If soil erosion of the bare or vegetation-protected slopes under different climate change scenarios are compared, the erosion modulus of the RCP 8.5 is the smallest and that of the RCP 2.6 is the largest. That may be related to the precipitation amount and its seasonal distribution. Firstly, the climate scenario of RCP 2.6 has the largest increase in precipitation amount, and that of RCP 8.5 has the least. Secondly, from the seasonal distribution of precipitation, the months with increasing precipitation of RCP 2.6 are mainly at the beginning of the vegetation growing season (i.e., June (19.98 mm) and July (14.58 mm)), and that of RCP 8.5 is mainly September (26.73 mm), which already towards the end of the vegetation growing season. The mismatch of increasing precipitation and vegetation growth of RCP 2.6 increases soil erosion.

4.4. To be improved in future research

This paper quantified the soil erosion and slope stability of different combination scenarios with the WEPP model and FLAC/Slope software. We tried to ensure the acceptability of the estimated results by means of multiple GCMs and validation of the WEPP model with field experiments and relative research. However, there are some insufficient to be improved in future research.

Firstly, future research needs to explore the adaption of land consolidation to extreme rainfall. Not only precipitation amount but individual rainstorm events and rainfall intensity affect soil erosion (Liu et al., 2022; Yue et al., 2020), but it remains challenging to predict future rainfall intensity with observational data based on stochastic weather generator (Wang et al., 2018; Yin and Chen, 2020). The impact of existing extreme rainfall on land consolidation will be strengthened in future research.

Secondly, future research needs to explore the validation of the model with slopes protected by more vegetation types. The WEPP model was widely used in soil erosion areas around the world (Borrelli et al., 2021), and this paper validated the model with field experiments and compared estimated results with relative studies. However, there was no validated data on the slopes with vegetation protection, and the number of vegetation types was not enough, which will be strengthened in future research.

Thirdly, future research needs to explore the calculation of the safety factor with the impact of climate change and vegetation. The slope stability was quantified with the safety factor using FLAC/Slope software which was widely used in international geotechnical communities (Chugh et al., 2007). However, the safety factor is difficult to validate. This paper also did not consider the effect of climate change and vegetation on the safety factor. Rainfall can weaken the slope stability, and vegetation has complex effects on slope stability, mainly manifested in the enhancement of the stability of the root system, and the weakening of the stability of the vegetation weight, wind, and water storage (Kokutse et al., 2016; Kim et al., 2017; Emadi-Tafti et al., 2021).

5. Conclusions

A construction site (e.g., roads, railways, mining areas, and water conservancy engineering) generally undergoes problems like vegetation destruction, landscape degradation, soil loss, and landslide, especially the high and steep slopes of a construction site. It is difficult for present research of observation experiments and investigation to deal with these problems under climate change. To alleviate soil erosion and slope instability of construction sites, this research proposed an optimal

method for designing slope inclination and vegetation planting, mainly including scenarios design, model calculation, and scheme optimization. By selecting a back catchment in Yangjuangou catchment of Yan'an City, Shaanxi Province as a case study, the paper designed 54 combined scenarios consisting of 6 slopes, 3 types of vegetation (including bare land), and 3 climate scenarios. Then, we quantified soil erosion and slope stability under different scenarios using FLAC/Slope software and Water Erosion Prediction Project (WEPP) model. Finally, we innovatively designed elasticity indicators to trade off the increase of the flat land area formed by land consolidation and the resulting reduction in slope stability and increase in soil erosion.

The main findings are as follows. (1) The future climate showed a trend of "warm and humid". Each month average of the predicted daily maximum and minimum temperature under the three climate change scenarios (i.e., RCP 2.6, RCP 4.5, and RCP 8.5) during 2020-2050 is higher than that during 1971-2005, and the predicted annual precipitation under three climate change scenarios during 2020-2050 are 41.48 mm, 37.35 mm, and 37.21 mm higher than the historical measured data during 1971-2005. (2) The erosion modulus of the bare slopes decreases with the increase of slope inclination under the 3 scenarios, but that of the vegetated slopes showed an inverse trend. Caragana microphylla demonstrated a stronger ability of soil conservation than Amorpha fruticosa. The soil erosion caused by the increases of the excavation slope increases significantly when the slope is greater than 53°. (3) The value of the safety factor decreases with the increase of slope inclination, and it is higher than 1.0 when the inclinations are below 73°. The slope stability caused by the increases in the excavation slope decreases obviously when the slope is greater than 53°. (4) With the elasticity indicators, it was found that the slope of 53° with Caragana microphylla could be the optimal combination scheme considering flat land creating and the safety of slopes. The technical process and the resulting factor could support maintaining a safe ecological environment of construction sites. The optimal combination scheme needed to be adjusted based on the detailed data of project areas.

Declaration of Competing Interest

The authors declare that they have no known competing financial interests or personal relationships that could have appeared to influence the work reported in this paper.

Data availability

Data will be made available on request.

Acknowledgements

This study was supported by National Key Research and Development Program of China (Grant Nos. 2017YFC0504701) and National Natural Science Foundation of China (Grant Nos. 41801175).

References

Borrelli, P., Alewell, C., Alvarez, P., Anache, J.A.A., Baartman, J., Ballabio, C., Bezak, N., Biddoccu, M., Cerdà, A., Chalise, D., Chen, S., Chen, W., De Girolamo, A.M., Gessesse, G.D., Deumlich, D., Diodato, N., Efthimiou, N., Erpul, G., Fiener, P., Freppaz, M., Gentile, F., Gericke, A., Haregeweyn, N., Hu, B., Jeanneau, A., Kaffas, K., Kiani-Harchegani, M., Villuendas, I.L., Li, C., Lombardo, L., López-Vicente, M., Lucas-Borja, M.E., Märker, M., Matthews, F., Miao, C., Mikoš, M., Modugno, S., Möller, M., Naipal, V., Nearing, M., Owusu, S., Panday, D., Patault, E., Patriche, C.V., Poggio, L., Portes, R., Quijano, L., Rahdari, M.R., Renima, M., Ricci, G.F., Rodrigo-Comino, J., Saia, S., Samani, A.N., Schillaci, C., Syrris, V., Kim, H.S., Spinola, D.N., Oliveira, P.T., Teng, H., Thapa, R., Vantas, K., Vieira, D., Yang, J.E., Yin, S., Zema, D.A., Zhao, G., Panagos, P., 2021. Soil erosion modelling: A global review and statistical analysis. Sci. Total Environ. 780, 146494 https://doi.org/10.1016/j.scitoteny.2021.146494.

Browning, E.K., Zupan, M.A., 2020. Microeconomics: Theory and applications. John Wiley & Sons.

Cao, Z., Liu, Y., Li, Y., 2022. Rural transition in the loess hilly and gully region: From the perspective of "flowing" cropland. Journal of Rural Studies 93, 326–335. https://doi. org/10.1016/j.jrurstud.2019.04.003.

- Chen, J., Zhang, X.J., Li, X., 2018. A Weather Generator-Based Statistical Downscaling Tool for Site-Specific Assessment of Climate Change Impacts. Trans. ASABE 61, 977–993. https://doi.org/10.13031/trans.12601.
- Chugh, A.K., Stark, T.D., DeJong, K.A., 2007. Reanalysis of a municipal landfill slope failure near Cincinnati, Ohio, USA. Can. Geotech. J. 44 (1), 33–53.
- Douglas-Mankin, K.R., Roy, S.K., Sheshukov, A.Y., Biswas, A., Gharabaghi, B., Binns, A., Rudra, R., Shrestha, N.K., Daggupati, P., 2020. A comprehensive review of ephemeral gully erosion models. CATENA 195, 104901. https://doi.org/10.1016/j.catena.2020.104901.
- Du, M., 2013. Root structure characteristics and spatial heterogeneity of different-plantage of Amorpha. Lanzhou University, Lanzhou in Chinese with English abstract.
- Emadi-Tafti, M., Ataie-Ashtiani, B., Hosseini, S.M., 2021. Integrated impacts of vegetation and soil type on slope stability: A case study of Kheyrud Forest. Iran. Ecological Modelling 446, 109498.
- Feng, W., Liu, Y., Chen, Z., Li, Y., Huang, Y., 2022. Theoretical and practical research into excavation slope protection for agricultural geographical engineering in the Loess Plateau: A case study of China's Yangjuangou catchment. Journal of Rural Studies 93, 309–317. https://doi.org/10.1016/j.jrurstud.2019.01.020.
- Flanagan, D.C., Frankenberger, J.R., Ascough II, J.C., 2012. WEPP: model use, calibration, and validation. Trans. ASABE 55 (4), 1463–1477. https://doi.org/10.13031/2013.42254.
- Fu, B., Chen, L., Ma, K., 1999. The effect of land use change on the reginal environment in the Yangjuangou catchment in the loess plateau of China. Acta Geographica Sinica 54, 241–246 in Chinese with English abstract.
- Gao, X., Zhao, Q., Zhao, X., Wu, P., Pan, W., Gao, X., Sun, M., 2017. Temporal and spatial evolution of the standardized precipitation evapotranspiration index (SPEI) in the Loess Plateau under climate change from 2001 to 2050. Sci. Total Environ. 595, 191–200. https://doi.org/10.1016/j.scitotenv.2017.03.226.
- Hancock, G.R., Lowry, J.B.C., Saynor, M.J., 2016. Early landscape evolution A field and modelling assessment for a post-mining landform. CATENA 147, 699–708. https://doi.org/10.1016/j.catena.2016.08.015.
- He, C.-X., 2015. The situation, characteristics and effect of the Gully Reclamation Project in Yan'an, Journal of Earth Environment 6, 255–260.
- Hou, X., Cao, Q., 1990. Study on the benefits of plants to reduce sediment in the loess rolling gullied region of north Shaanxi. Bulletin of Soil and Water Conservation 10 (2), 33–40 in Chinese with English abstract.
- Hu, Y., Gao, M., Batunacun, 2020. Evaluations of water yield and soil erosion in the Shaanxi-Gansu Loess Plateau under different land use and climate change scenarios. Environmental Development 34, 100488. https://doi.org/10.1016/j. envdev.2019.100488.
- Huang, E., 1986. Cultivation and utilization of *Amorpha fruticosa*. China Forestry Publishing House, Beijing in Chinese with English abstract.
- Ipcc, 2013. Climate Change 2013: The Physical Science Basis. Cambridge University
- Jiang, F., Huang, Y., Wang, M., Lin, J., Zhao, G., Ge, H., 2014. Effects of Rainfall Intensity and Slope Gradient on Steep Colluvial Deposit Erosion in Southeast China. Soil Sci. Soc. Am. J. 78, 1741–1752. https://doi.org/10.2136/sssaj2014.04.0132.
- Jin, Z., Guo, L., Wang, Y., Yu, Y., Lin, H., Chen, Y., Chu, G., Zhang, J., Zhang, N., 2019. Valley reshaping and damming induce water table rise and soil salinization on the Chinese Loess Plateau. Geoderma 339, 115–125. https://doi.org/10.1016/j.geoderma.2018.12.048.
- Jourgholami, M., Karami, S., Tavankar, F., Lo Monaco, A., Picchio, R., 2021. Effects of slope gradient on runoff and sediment yield on machine-induced compacted soil in temperate forests. Forests 12, 49. https://doi.org/10.3390/f12010049.
- temperate forests. Forests 12, 49. https://doi.org/10.3390/f12010049.

 Kaya, A., Alemdağ, S., Dağ, S., Gürocak, Z., 2016. Stability assessment of high-steep cut slope debris on a landslide (Gumushane, NE Turkey). Bull. Eng. Geol. Environ. 75

 (1), 89–99. https://doi.org/10.1007/s10064-015-0753-6.
- Kim, J.H., Fourcaud, T., Jourdan, C., Maeght, J.-L., Mao, Z., Metayer, J., Meylan, L., Pierret, A., Rapidel, B., Roupsard, O., de Rouw, A., Sanchez, M.V., Wang, Y., Stokes, A., 2017. Vegetation as a driver of temporal variations in slope stability: The impact of hydrological processes: Variable Stability of Vegetated Slopes. Geophys. Res. Lett. 44, 4897–4907. https://doi.org/10.1002/2017GL073174.
- Kokutse, N.K., Temgoua, A.G.T., Kavazović, Z., 2016. Slope stability and vegetation: Conceptual and numerical investigation of mechanical effects. Ecol. Eng. 86, 146–153.
- Laflen, J.M., Elliot, W.J., Flanagan, D.C., Meyer, C.R., Nearing, M.A., 1997. WEPP-predicting water erosion using a process-based model. J. Soil Water Conserv. 52 (2), 96–102
- Lee, G., McLaughlin, R.A., Whitely, K.D., Brown, V.K., 2018. Evaluation of seven mulch treatments for erosion control and vegetation establishment on steep slopes. J. Soil Water Conserv. 73 (4), 434–442. https://doi.org/10.2489/jswc.73.4.434.
- Li, T., Zhao, L., Duan, H., Yang, Y., Wang, Y., Wu., F., 2020. Exploring the interaction of surface roughness and slope gradient in controlling rates of soil loss from sloping farmland on the Loess Plateau of China. Hydrological Processes, 34(2), 339-354. https://doi.org/10.1002/hyp.13588.
- Li, X., Gao, J., Guo, Z., Yin, Y., Zhang, X., Sun, P., Gao, Z., 2020b. A Study of Rainfall-Runoff Movement Process on High and Steep Slopes Affected by Double Turbulence Sources. Sci. Rep. 10, 9001. https://doi.org/10.1038/s41598-020-66060-3.
- Li, P., Qian, H., Wu, J., 2014. Environment: Accelerate research on land creation. Nature 510, 29–31. https://doi.org/10.1038/510029a.
- Li, Y., Zhang, X., Cao, Z., Liu, Z., Lu, Z., Liu, Y., 2021. Towards the progress of ecological restoration and economic development in China's Loess Plateau and strategy for

- more sustainable development. Sci. Total Environ. 756, 143676. https://doi.org/10.1016/j.scitotenv.2020.143676.
- Liang, Y., Long, Z., 2010. Cultivation theory and techniques for Robinia pseudoacacia L. China Forestry Publishing House, Beijing in Chinese with English abstract.
- Liu, Y., Li, Y., 2014. China's land creation project stands firm. Nature 511, 410. https://doi.org/10.1038/511410c.
- Liu, Y., Li, Y., 2017. Engineering philosophy and design scheme of gully land consolidation in Loess Plateau. Transactions of the Chinese Society of Agricultural Engineering 33 (10), 1–9 in Chinese with English abstract.
- Liu, Y., Guo, Y., Li, Y., Li, Y., 2015. GIS-based effect assessment of soil erosion before and after gully land consolidation: A case study of Wangjiagou project region, Loess Plateau. Chin. Geogr. Sci. 25, 137–146. https://doi.org/10.1007/s11769-015-0742-5
- Liu, Y., Chen, Z., Li, Y., Feng, W., Cao, Z., 2017. The planting technology and industrial development prospects of forage rape in the loess hilly area: A case study of newlyincreased cultivated land through gully land consolidation in Yan'an, Shaanxi Province. Journal of Natural Resources 32, 2065–2074 in Chinese with English abstract
- Liu, J., Gao, G., Wang, S., Fu, B., 2019b. Combined effects of rainfall regime and plot length on runoff and soil loss in the Loess Plateau of China. Earth and Environmental Science Transactions of the Royal Society of Edinburgh 109, 397–406. https://doi. org/10.1017/S1755691018000531.
- Liu, G., Hu, F., Zheng, F., Zhang, Q., 2019a. Effects and mechanisms of erosion control techniques on stairstep cut-slopes. Sci. Total Environ. 656, 307–315. https://doi. org/10.1016/j.scitotenv.2018.11.385.
- Liu, J., Liang, Y., Gao, G., Dunkerley, D., Fu, B., 2022. Quantifying the effects of rainfall intensity fluctuation on runoff and soil loss: From indicators to models. J. Hydrol. 607, 127494 https://doi.org/10.1016/j.jhydrol.2022.127494.
- Liu, B., Qu, J., Wagner, L.E., 2013. Building Chinese wind data for Wind Erosion Prediction System using surrogate US data. J. Soil Water Conserv. 68, 104A–107A. https://doi.org/10.2489/jswc.68.4.104A.
- Liu, J.-E., Zhang, X., Zhou, Z., 2019c. Quantifying effects of root systems of planted and natural vegetation on rill detachment and erodibility of a loessial soil. Soil Tillage Res. 195, 104420 https://doi.org/10.1016/j.still.2019.104420.
- Ma, L., Liu, L., Niu, Z., Yue, J., Zhao, Y., Jin, J., Chang, Y., 2019. Ecological and economic benefits of planting winter rapeseed (Brassica rapa L.) in the wind erosion area of northern China. Sci. Rep. 9, 20272.
- Miao, C., He, B., Chen, X., Wu, Y., 2004. Study on the application and contrast of CLIGEN and BPCDG in WEPP model application. Chinese Agricultural Science Bulletin 20 (6), 321–324 in Chinese with English abstact.
- Mohammad, A.G., Adam, M.A., 2010. The impact of vegetative cover type on runoff and soil erosion under different land uses. CATENA 81, 97–103. https://doi.org/ 10.1016/j.catena.2010.01.008.
- Murthy, V.N.S., 2003. Geotechnical engineering: Principles and practices of soil mechanics and foundation engineering. Marcel Dekke, New York.
- Navarro-Hevia, J., Lima-Farias, T.R., de Araújo, J.C., Osorio-Peláez, C., Pando, V., 2016. Soil erosion in steep road cut slopes in Palencia (Spain). Land Degrad. Dev. 27 (2), 190–199. https://doi.org/10.1002/ldr.2459.
- Nearing, M.A., Foster, G.R., Lane, L.J., Finkner, S.C., 1989. A process-based soil-erosion model for USDA-Water Erosion Prediction Project Technology. Trans. ASAE 32 (5), 1587–1593.
- Niu, X., 2003. Research on Caragana Microphylla. Science Press, Beijing in Chinese with English abstract.
- Qian, F., Cheng, D., Ding, W., Huang, J., Liu, J., 2016. Hydraulic characteristics and sediment generation on slope erosion in the Three Gorges Reservoir Area, China. Journal of Hydrology and Hydromechanics 64, 237–245. https://doi.org/10.1515/ jobb.2016.0029
- Ramos-Scharrón, C.E., Alicea-Díaz, E.E., Figueroa-Sánchez, Y.A., Viqueira-Ríos, R., 2022. Road cutslope erosion and control treatments in an actively-cultivated tropical montane setting. CATENA 209, 105814. https://doi.org/10.1016/j. catena.2021.105814.
- Samtani, N.C., Nowatzki, E.A., 2006. Soils and Foundations Reference Manual Volume 1, 20590
- Satyanarayana, I., Budi, G., Murmu, S., 2021. Stability analysis of a deep highwall slope using numerical modelling and statistical approach—a case study. Arab J Geosci 14, 179. https://doi.org/10/gpg7b6.

- Shan, Y., Xie, J., Lei, N., Dong, Q., 2020. Soil Moisture Characteristics of a Typical Slope in the Watershed of the Loess Plateau for Gully Land Consolidation Project. E3S Web Conf. 199, 00006. https://doi.org/10.1051/e3sconf/202019900006.
- Shi, W., Huang, M., Barbour, S.L., 2018. Storm-based CSLE that incorporates the estimated runoff for soil loss prediction on the Chinese Loess Plateau. Soil Tillage Res. 180, 137–147. https://doi.org/10.1016/j.still.2018.03.001.
- Shinohara, K., Oida, M., Golman, B., 2000. Effect of particle shape on angle of internal friction by triaxial compression test. Power Technology 107, 131–136. https://doi. org/10/dvdfdh.
- Singh, T.N., Pradhan, S.P., Vishal, V., 2013. Stability of slopes in a fire-prone mine in Jharia Coalfield, India. Arab J Geosci 6, 419–427. https://doi.org/10/fgbmnc.
- Song, X., Sun, H., Xiao, X., Long, F., 2014. A study on the germination characteristics of 13 species plants for slope protection. Seed 33 (5), 1–7 in Chinese with English abstract.
- Taylor, K.E., Stouffer, R.J., Meehl, G.A., 2012. An Overview of CMIP5 and the Experiment Design. Bull. Am. Meteorol. Soc. 93, 485–498. https://doi.org/10.1175/ BAMS-D-11-00094.1.
- Wang, L., Dalabay, N., Lu, P., Wu, F., 2017. Effects of tillage practices and slope on runoff and erosion of soil from the Loess Plateau, China, subjected to simulated rainfall. Soil Tillage Res. 166, 147–156. https://doi.org/10.1016/j.still.2016.09.007.
- Wang, M., Liu, Q., Pang, X., 2021. Evaluating ecological effects of roadside slope restoration techniques: A global meta-analysis. J. Environ. Manage. 281, 111867 https://doi.org/10.1016/j.jenvman.2020.111867.
- Wang, W., Yin, S., Flanagan, D.C., Yu, B., 2018. Comparing CLIGEN-Generated Storm Patterns with 1-Minute and Hourly Precipitation Data from China. Journal of Applied Meteorology and Climatology 57, 2005–2017. https://doi.org/10.1175/ JAMC-D-18-0079.1.
- Wang, X., Zhuo, L., Li, C., Engel, B.A., Sun, S., Wang, Y., 2020. Temporal and spatial evolution trends of drought in northern Shaanxi of China: 1960–2100. Theor. Appl. Climatol. 139, 965–979. https://doi.org/10.1007/s00704-019-03024-2.
- Wei, Y., Miao, H., Ouyang, Z., Chen, L., Gui, L., 2004. Evaluation of the economic and ecological efficiencies of the four shrubs in hilly areas of the Loess Plateau. Agricultural Research in the Arid Areas 22 (4), 158–162 in Chinese with English abstract.
- Xu, Q., Chen, W., Zhao, K., Zhou, X., Du, P., Guo, C., Ju, Y., Pu, C., 2021. Effects of landuse management on soil erosion: A case study in a typical watershed of the hilly and gully region on the Loess Plateau of China. CATENA 206, 105551. https://doi.org/ 10.1016/j.catena.2021.105551.
- Xue, S., Li, Z., Li, P., Liu, G., Dai, Q., 2009. Effects of different vegetation restoration models on soil anti-erodibility in loess hilly area. Transactions of the Chinese Society of Agricultural Engineering 25 (S1), 69–72 in Chinese with English abstract.
- Yin, S., Chen, D., 2020. Weather generators. In Oxford Research Encyclopedia of Climate Science.
- Yin, J., Qiu, G., He, F., He, K., Tian, J., Zhang, W., Xiong, Y., Zhao, S., Liu, J., 2008. Leaf area characteristics of plantation stands in semi-arid loess hilly-gully region of China. Journal of Plant Ecology 32 (2), 440–447 in Chinese with English abstract.
- Yue, L., Juying, J., Bingzhe, T., Binting, C., Hang, L., 2020. Response of runoff and soil erosion to erosive rainstorm events and vegetation restoration on abandoned slope farmland in the Loess Plateau region. China. Journal of Hydrology 584, 124694. https://doi.org/10.1016/j.jhydrol.2020.124694.
- Zhang, G., 2004. Adaptability of climate generator of CLIGEN in Yellow River Basin.

 J. Soil Water Conserv. 18(1), 175–178, 196 in Chinese with English abstract.
- Zhang, C.-B., Chen, L.-H., Liu, Y.-P., Ji, X.-D., Liu, X.-P., 2010. Triaxial compression test of soil-root composites to evaluate influence of roots on soil shear strength. Ecological Engineering 36, 19–26. https://doi.org/10/cgrshn.
- Zhang, X.C., Liu, W.Z., 2005. Simulating potential response of hydrology, soil erosion, and crop productivity to climate change in Changwu tableland region on the Loess Plateau of China. Agric. For. Meteorol. 131, 127–142. https://doi.org/10.1016/j.agrformet.2005.05.005.
- Zhang, X., Song, J., Wang, Y., Deng, W., Liu, Y., 2021. Effects of land use on slope runoff and soil loss in the Loess Plateau of China: A meta-analysis. Sci. Total Environ. 755, 142418 https://doi.org/10.1016/j.scitotenv.2020.142418.
- Zhang, B., Zhang, G., Yang, H., Wang, H., Li, N., 2018. Soil erodibility affected by vegetation restoration on steep gully slopes on the Loess Plateau of China. Soil Res. 56, 712–723. https://doi.org/10.1071/SR18129.